

Melanin and melanoma: Updating molecular structure and photothermal therapy

Melanina y melanoma: Actualización de la estructura molecular y terapia fototérmica

STOCKERT, JC^{1,2}

¹Universidad de Buenos Aires, Facultad de Ciencias Veterinarias, Instituto de Investigación y Tecnología en Reproducción Animal, Avda. Chorroarín 280, Buenos Aires C1427CWO.

²Universidad de Buenos Aires, Facultad de Medicina, Instituto de Oncología “Angel H. Roffo”, Area Investigación, Avda. San Martín 5481, Buenos Aires C1417DTB, Argentina.

SUMMARY

Melanin pigment and melanoma are two fields of increasing interest and relevance in biomedical research. Melanins are ubiquitous biopigments with strong adaptive value and multiple functions. In mammals, melanin corresponds to eumelanin (brown-black) and pheomelanin (yellow-red), and is found mainly in the skin and derivatives, retinal pigmented epithelium, and central nervous systems (neuromelanin, in *substantia nigra*, *locus coeruleus*, etc.). Melanin also occurs in the malignant melanoma, which is one of the most aggressive and therapy-resistant tumors in veterinary and human medicine. Several chemical structures have been proposed for eumelanin, but there is still no agreement about its molecular organization. Two models, namely a flexible linear chain, and a rigid planar chain, are the structures that better agree with physico-chemical properties of eumelanin. The latter model, which appears as the most plausible structure, corresponds to a benzoquinone derivative of the porphycene ring, and explains the broad-band light absorption, antioxidant capacity, electric conductivity, and photothermal effect, as well as the multilayered and graphite-like organization shown by X-ray crystallography and electron microscopy. In addition to traditional oncologic treatments and recent immunological and gene therapy advances, photodynamic and photothermal approaches represent novel therapeutic modalities for melanoma. In the latter case, since eumelanin is practically the ideal photothermal sensitizer, the massive vibrational decay from photo-excited electronic states after NIR irradiation induces an immediate and highly efficient heating response that results in coagulative necrosis of the tumor. This allows repetitive treatments due to the remaining melanin contained in tumoral melanophages. Although the evolution and prognosis of the advanced melanoma is still a concern, new physical procedures can now be applied.

Keywords: (antitumor therapy), (eumelanin), (indole polymers), (melanoma), (photothermal therapy).

RESUMEN

La melanina y el melanoma son dos campos de interés y relevancia crecientes en investigación biomédica. Las melaninas son biopigmentos ubicuos con gran valor adaptativo y múltiples funciones. En mamíferos, la melanina corresponde a la eumelanina (marrón-negro) y a la feomelanina (amarillo-rojo), y se encuentra en la piel y derivados, epitelio pigmentado de la retina, y sistema nervioso central (neuromelanina, en *substantia nigra*, *locus coeruleus*, etc). La melanina también está presente en el melanoma maligno, uno de los tumores más agresivos y resistentes a la terapia en medicina veterinaria y humana. Varias estructuras químicas han sido propuestas para la eumelanina, pero todavía no hay acuerdo sobre su organización molecular. Dos modelos, uno constituido por una cadena lineal y flexible, y otro por una cadena plana y rígida son las estructuras que mejor encajan con las propiedades físico-químicas de la eumelanina. El último modelo, que parece ser la estructura más plausible, corresponde a un derivado benzoquinónico del porfírico y explica la absorción de luz de banda ancha, la capacidad antioxidante, la conductividad eléctrica y el efecto fototérmico, así como también la organización en multicapa similar al grafito mostrada por la cristalografía de rayos X y la microscopía electrónica. Sumados a los tratamientos oncológicos tradicionales y a los avances inmunológicos y de terapia génica más recientes, los abordajes fotodinámico y fototérmico representan novedosas modalidades terapéuticas para el melanoma. En este último caso, como la eumelanina es el sensibilizador fototérmico prácticamente ideal, el decaimiento vibracional masivo a partir de estados electrónicos foto-excitados por NIR induce un calentamiento inmediato y muy eficiente que produce la necrosis coagulativa del tumor. Esta respuesta permite tratamientos repetidos debido a la melanina remanente contenida en los melanófagos tumorales. Aunque la evolución y pronóstico del melanoma avanzado son todavía asuntos preocupantes, nuevos procedimientos físicos pueden ser ahora aplicados.

Palabras clave: (eumelanina), (fototerapia), (melanoma), (polímeros de indol), (terapia antitumoral).

INTRODUCTION

Melanins are probably the most ancient group of natural pigments (biochromes), with multiple roles in almost all organisms across the Phyla. Prokaryota and Eukaryota^{30,35,81}, the last including the kingdoms Protista, Fungi, Plantae, and Animalia have melanins. Melanins are indole- and catechol-type biopolymers, and in mammals, indole-containing melanins correspond to eumelanin (brown-black) and pheomelanin (yellow-red). They are found mainly in the skin and derivatives, retinal pigmented epithelium, and central nervous system as neuromelanin (e.g., *substantia nigra*, *locus coeruleus*, and *stria vascularis* in the cochlea). In plants and fungi, melanins generally correspond to the catechol-type and they are named allomelanins¹²⁹. Recent reviews deal with the main features of melanin and melanoma^{14,81,82}.

The precise molecular structure of eumelanins is still poorly known, although an overwhelming evidence indicates that they are formed by polymers with high conjugation (double bond) de-

gree^{14,35}. On account of the close relation between chemical organization and eumelanin properties, in the present review emphasis will be made on the molecular structure, as well as on the high photon absorption and heat production, which results in the known and useful photothermal effect^{58,94}.

Eumelanin occurs as granules about 1 μm in diameter (melanosomes) produced in neuro-ectodermal melanocytes. The malignant melanoma, one of the most aggressive animal tumors, just originates from this cell type. In veterinary medicine, in addition to experimental animals (e.g., mice, hamsters)^{20,67,91,110}, melanoma tumors also occur in dogs, horses, and in companion and larger domestic animals^{42,43,109}. In dogs and humans, melanoma is a malignancy very aggressive and highly resistant to standard treatments, with a significant overlapping to humans in both clinical and histopathological features. Spontaneous canine melanoma is also a more suitable disease model of human melanoma than traditional murine systems, providing useful preclinical data for translation of treatment to human patients.

On account of the difficulty in successfully treating the malignant melanoma in advanced and metastatic stage^{3,71}, further studies on new therapeutic modalities based on chemical and physical approaches are still necessary. At present, new protocols using cytokines, check point and kinase inhibitors, gene and immunotherapy are applied for advanced melanomas^{2,12,25,36,43,121,104}. However, photochemical and photophysical treatments are also increasingly employed, and examples are the photodynamic- and photothermal therapies¹⁴. The aim of this review is to update and summarize proposed molecular structures of eumelanin, as well as macromolecular properties, mainly to fundament therapeutic developments for its use as an ideal endogenous chromophore for physical therapy of melanomas.

CHEMICAL STRUCTURE

The chemical structure of eumelanin has been commonly investigated by the analysis of fragmented degradation products, and less attention has been devoted to the application of physical methods. Studies based on X-ray crystallography and electron microscopy have now shown that synthetic and natural eumelanin present a multilayer graphite-like organization, which explains most physico-chemical properties of this supramolecular solid material. Several molecular models have been suggested for eumelanin, from simple aggregates of indole monomers³⁸ to cyclic²³ or helicoidal tetramers⁸⁴, and flexible linear or zig-zag chain polymers⁸⁶. Common eumelanin models from known indole precursors such as 5,6-dihydroxyindole (DHI), and indolequinone (IQ) have been recently reviewed¹⁴.

In general, three types of molecular organization can be taken into account, namely monomer and cyclic oligomers, flexible chains, and rigid chains. There are supports and opposing views for each of these structural models, in order to explain the striking properties of eumelanin. Only flexible and rigid chain types will be described here (Figure 1). Exploring theoretical structures by molecular modeling has allowed advances in understanding the organization of natural and synthetic melanins.

Poly 2-4 IQ zig-zag chain, as well as linear poly DHICA (Figure 1 A) and poly 4-7 IQ chains are flexible polymers, which represent the commonly formulated structures of eumelanin^{35,72,92}. In the case of tetra 4-7 IQ (Figure 2,A), a dihedral angle of $\sim 40^\circ$

between IQ units appears as an impediment to the electron π conjugation. However, this dihedral angle becomes lower ($\sim 20^\circ$) in the first excited state (S_1) of stacked IQ rings, thus allowing increased resonance. The 3D organization of common eumelanin models is still poorly known, and there are different views according to the polymer structure. Stacking of flexible linear or zig-zag chains^{35,72}, or bundling arrays of flexible linear polymers have been proposed^{186,92}.

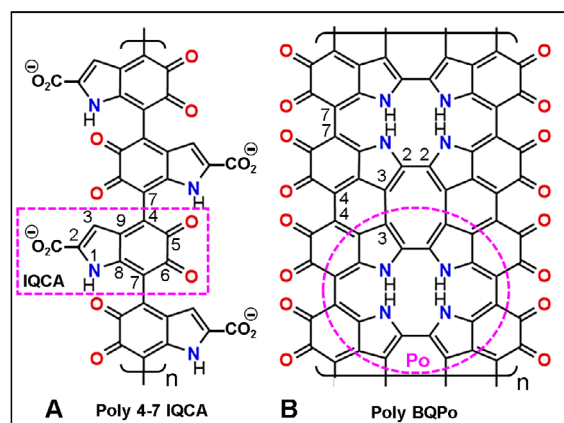


Figure 1. Common models of eumelanin polymers formed by indolequinone units showing formal double bonds and atom numbering. A: linear flexible chain of poly 4-7 indolequinone carboxylic acid (IQCA, violet rectangle). B: planar rigid poly benzoquinone-porphycene (poly BQPo, with the porphycene ring (Po) as a violet ellipse). Chemical structures are represented according the indicated references, poly 4-7 IQCA^{35,72,92}, and poly BQPo⁹⁰. In this review, all indoles are shown in their oxidized form (IQ).

Other chemical structures have been suggested as rigid models. A planar poly 1-7,3-4 IQ^{85,126}, and a curved fused IQ (poly 2-7,3-4 IQ) are rigid models that could explain several physico-chemical properties of eumelanin. The structure and resonance of zig-zag 2-4 IQ and 4-7 IQ models have been recently reviewed¹⁴.

Interestingly, an overlooked double IQ chain model for eumelanin was early proposed⁹⁰. In this polymer, formulated as poly 2-2,3-3,4-4,7-7 IQ, or simply, poly BQPo, the monomeric unit is a tetra-benzoquinone (BQ) derivative of the porphycene ring (Po) (Figure 1,B), which is a known porphyrin isomer¹¹⁵. The porphycene ring and several metal complexes are planar unsaturated macrocycles, and therefore, their polymers must be highly conjugated and stacked structures

that share important physico-chemical properties with graphite-like solid state materials.

The possibility that this planar benzoquinone-porphycene (BQPo) unit (Figures 1,B and 3,A) could be the main component of both eumelanin and synthetic melanins is very interesting. Some authors have mentioned that eumelanin could be formed by this BQPo unit or other similar ones^{7,15,26,126}. In contrast with linear or zig-zag flexible chain models such as poly 4-7 IQ and 2-4 IQ³⁵, the planar poly BQPo model fulfills most characteristics of eumelanin as a supramolecular solid based on stacked 3D multilayers, explaining its broad-band absorption, semi- and photo-conductivity, fast electronic energy decay with efficient heat production, binding affinity for aromatic ligands, as well as ultrastructural and crystallographic features.

MOLECULAR ORBITALS

Inspection of molecular orbital (MOs) of melanin models allows to explain the conjugation changes induced by photoexcitation. A tetrameric portion of the poly 4-7 IQ model is shown in Figure 2,A. Ground and light-excited singlet states of molecules (S_0 and S_1 , respectively) result in different MOs, which correspond to the highest-occupied (HOMO), and lowest-unoccupied (LUMO) energy levels, respectively^{14,113}.

In this case, the S_1 state (LUMO+0) of the 4-7 IQ tetramer has a more extended electron π conjugation than that of the ground singlet S_0 state (HOMO-0), showing a larger and continuous extension of green and violet lobes in Figure 2,C. In models of melanin polymers, excited states are better represented by mesomeric ionic forms, with MOs showing the high π^* conjugation degree (Figure 2,D)¹⁴. The massive dissipation of the electronic energy from excited MOs produces a great amount of heat, namely, a photothermal response.

In the case of the tetra BQPo model (Figure 3), different MO orientations are also present. No preferential HOMO-0 orientation is observed, but a clear longitudinal direction can be seen in LUMO+0 (Figure 3,A,B). In this structure, the vicinal carbonyls (=HC-CO-CO-CH=) from *ortho*-benzoquinones show the same longitudinal LUMO+0 pattern as in poly 4-7 IQ. Likewise, the energy levels of excited states result

in a compact overlapping of the LUMO block, appearing similar to the electron conduction band of semiconductors.

Quinone compounds present as building units of allomelanins also show the same extended LUMO pattern. The increase of absorption and dark color of the DHI-melanin chromophore by further oxidation is explained by conversion of catechols to quinones^{86,92}. It seems logical to assume that, in pigments with increased number of linear *ortho*-benzoquinones, black color and broad-band absorption spectra are closely related to the high π^* -conjugation and extended longitudinal LUMO+0 components, with reduction of the HOMO-LUMO energy gap (increased semiconductor-like behavior).

SUPRAMOLECULAR PROPERTIES

Melanins have a great importance in biomedical fields and materials science due to their striking features: (a) broad-band light absorption spanning the ultraviolet (UV), visible, and near-infrared (NIR) spectrum; (b) semi-conductivity and photo-conductivity; (c) ultrasound absorption; (d) efficient dissipation of the absorbed photon energy as heat; (e) antioxidant and radical-scavenger activity; (f) reversible redox behavior; (g) high adhesiveness, and (h) strong binding of metal cations, drugs and organic compounds. Excellent reviews on the chemistry, properties, and applications of melanin and melanin-like materials have been published^{19,30,34,35,45,54,82,111,93,106}. Light absorption from mammalian, invertebrate (cuttlefish), and synthetic (polydopamine) melanins have the same spectral characteristics^{86,96}, showing a monotonic broad-band absorption spectrum with exponential decay, as occurs in typical graphitic materials¹⁴. In addition to UV, visible and NIR light, eumelanin is capable of absorbing X- and γ -rays^{52,66}, as well as ultrasound in the 1-MHz range^{62,63,83}.

The broad-band photonic absorption of eumelanin reminds more to an inorganic semiconductor material with a small energy band gap (about 0.5-1.5 eV) than to an organic chromophore with absorption peaks typically associated to transitions from π bonding to antibonding π^* orbitals. Thus eumelanins and black graphitic materials are supramolecular structures and share the broad-band absorption that characterizes amorphous semiconductors with close valence and conduction bands^{82,89}. Interestingly, these features are

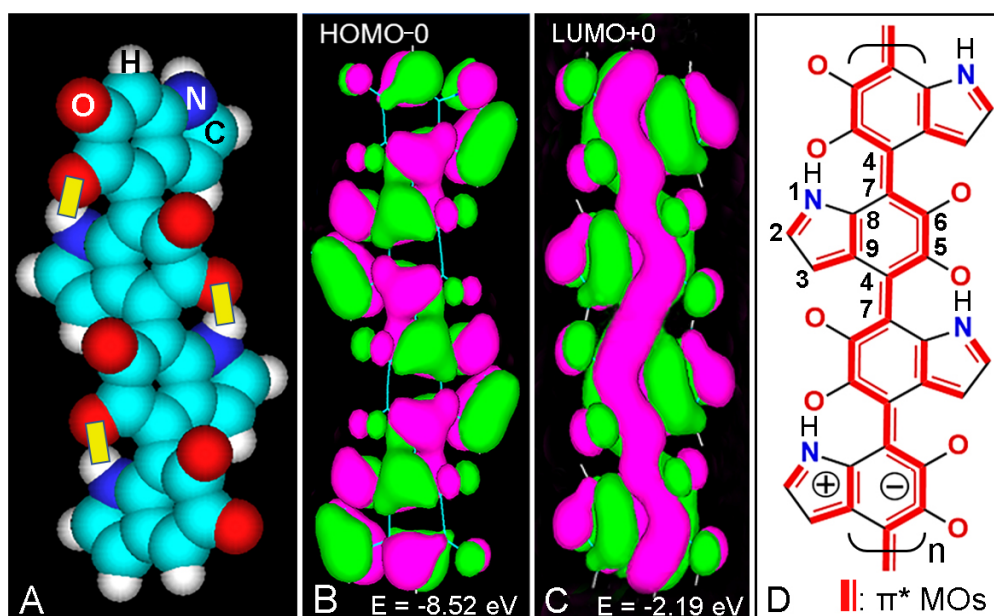


Figure 2. A: Atomic volume model of tetra 4-7 IQ. PM3 geometry optimization with HyperChem 7 by Polak-Riviere method converged to 0.1 kcal/(Å mol). H bonds of 2.7 Å are shown as yellow bars. Averaged dihedral angle between indole units: 40°. B, C: HOMO-0 and LUMO+0, respectively, of tetra 4-7 IQ showing positive (green) and negative (violet) π -orbital lobes (Gouraud shaded 3D isosurface), with energy values (E). Orbital contour (1/orbital radius): 0.02. D: Conjugated double bond pattern (red thick and thin lines) of poly 4-7 IQ in the S1 state, according to LUMO+0.

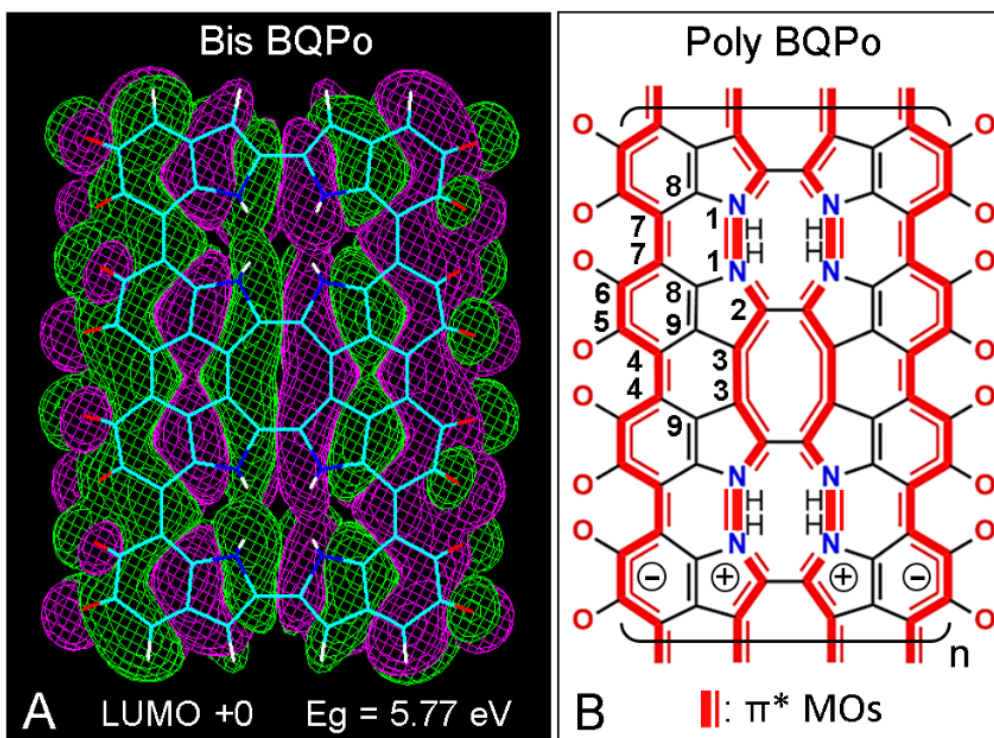


Figure 3. A: LUMO+0 pattern of bis BQPo, recorded as in Fig. 2. Jorgensen-Salem surface, orbital contour: 0.0008. Observe the long LUMO+0 orbital lobes that correspond to the conjugated double bond pattern of the S1 state. Energy gap (E_g) = 5.77 eV (from -8.81 eV to -3.04 eV. B: Chemical structure of poly BQPo, showing the conjugated double bond pattern (red thick and thin lines).

also found in pyrolyzed polydopamine (PDA) films, graphene, and PDA-based carbon spheres⁷⁷.

If a planar indole polymer such as poly BQPo would be the main structure of eumelanin, then a typical graphite-like organization of stacked aromatic layers would be found using transmission electron microscopy (TEM) and X-ray crystallography. In keeping with this, ultrastructural studies show that stacked multilayers with spacing of 3.4 Å is just the structural pattern observed in samples of natural and synthetic eumelanins (Figure 4)^{23,26,118,123}. It is difficult to conceive how other models (H-bound monomers, cyclic tetramers, zig-zag and linear flexible polymers) could explain the graphitic organization of eumelanin. In addition to planar structures, wavy, and concentrically stacked multilayers are commonly observed by TEM^{23,123}, which can be due to ether bridges that result in a curved organization of poly BQPo layers⁹⁰.

The conjugated structure of this polymer also allows easy redox changes and reversible equi-

librium between quinone and catechol groups. Eumelanin is a powerful antioxidant and detoxification agent by removing reactive oxygen species (ROS), oxidizing radicals, toxic heavy metals, and harmful chemicals which are relevant to body detoxification and protection. Among several unusual and intriguing features of eumelanin, its striking adhesivity and binding capacity to different surfaces and compounds are worth to note^{106,117}. Regarding the interaction with inorganic ions, eumelanin and synthetic melanins easily bind to mono-, di-, and trivalent metal cations such as Na, K, Mg, Ca, Al, Mn, Fe, Ni, Cu, Zn, Co, Cr, Cd, Sr, Ti, V, Mo, Ag, Sb, Hg, Pb, La, Gd, As, etc.^{35,45,89}.

Metal chelation by oxygen ligands such as carboxyl, catechol, and quinone groups could be responsible for side-to-side bridges between adjacent poly BQPo chains, as well as for strong adhesive binding to particles and surfaces^{24,77,103}. Likewise, chelation of heavy metal cations is possible mainly by nitrogen ligands of porphyrin or porphycene re-

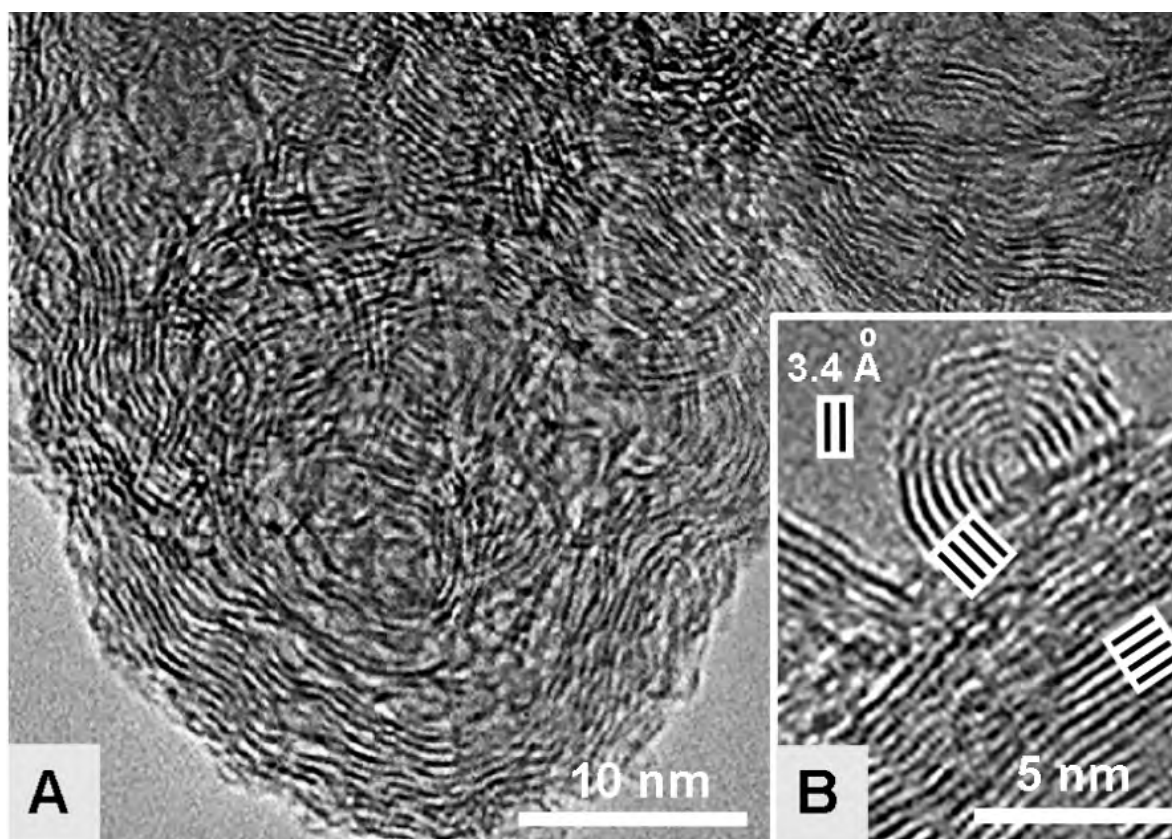


Figure 4. A: TEM image of synthetic polydopamine eumelanin, showing the wavy and/or concentric graphitic structure of the polymer layers. B: TEM image of the same material at higher magnification. Observe both the planar and curved (onion-like) stacked organization of the polymer, as well as the interlayer spacing of 3.4 Å between aromatic planes (Reproduced with permission from Chen et al., ACS Nano. 2013; 7: 1524-32).

gions (e.g., IQ tetramer, BQPo), and could provide the way for removing toxic metals. Eumelanin has reducing activity, and this feature is applied to reduce directly silver ion (Ag^+) to the uncharged metal (Ag^0)⁷⁷, which accounts for the argentaffin reaction to reveal melanin under the light microscope using the Fontana-Masson technique^{9,18}.

Due to the anionic character of eumelanin, it can be additionally stained by cationic dyes and complexes such as aluminum-hematein. However, dye binding to melanin could be also based on hydrophobic forces as occurs in the case of lipid stains. It is known that planar aromatic compounds can intercalate into adequate host lattices forming inclusion complexes¹²⁴. In the case of tissue components (polysaccharides, lignin, melanin, nucleic acids duplexes), bathochromic changes in the absorption spectra are induced by monomerization of dyes, which remain trapped between aliphatic chains or aromatic rings of the biopolymer^{6,112,114}. Fluorescence quenching is expected to occur in the case of fluorochromes intercalated into dark chromophores such as eumelanin, which can absorb emission by an inner filter (screen) effect, and therefore fluorescence reactions would be prevented¹¹³.

It is known that eumelanins are capable of dissipating >99.9% of absorbed UV- visible radiation through a non-radiative decay mode⁸⁵. Since the radiative decay of eumelanin is nearly zero, it is expected that its fluorescence emission should be negligible. However, an intriguing autofluorescence has been assigned to melanin^{40,46}, with an excitation peak at 450 nm and emissions from 440 nm to >800 nm, allowing autofluorescence lifetime imaging for ophthalmoscopy, detection of melanin in pigmented cells, and thermophoresis assays of melanin-binding drugs^{39,41,50}. However, previous UV irradiation or H_2O_2 oxidation are needed in order to induce visible eumelanin emission⁵⁹, which seems to occur by partial molecular degradation. It is worth to note that when the oxidized brown-black DAB polymer after immunoperoxidase method is subjected to UV irradiation, a strong yellowish fluorescence also appears due to degradation products⁴⁸. In the case of ophthalmoscopy, where the lifetime of autofluorescence from the retinal pigment epithelium is recorded, the most relevant autofluorescence is not due to melanin but to lipofuscin, and NAD(P)H, FAD, collagen, elastin, and carotenoids can be also involved³⁹.

PHOTOTHERAPY

In addition to immuno-, gene, and target-based treatments for melanoma, light-induced procedures are also applied. They include photodynamic therapy (PDT) and photothermal therapy (PTT). PDT is based on the administration of a photosensitizer (PS) drug that when irradiated with suitable light induces the formation of reactive oxygen species (ROS), which then provokes damage and death of tumor cells. The fundamentals and applications of PDT have been widely reviewed^{11,111,115,116,122,119}.

Melanoma PDT has been somewhat overlooked, possibly due to the strong light absorption of melanin and its anti-oxidant effect. However, there is now an increasing interest on PDT for melanoma, mainly using PSs such as methylene blue²², hypericin³¹, riboflavin⁴, chlorins^{95,107}, porphyrins^{101,108}, and phthalocyanins^{61,79,80,120}. Numerous *in vitro* and *in vivo* studies show considerable efficiency of PDT for melanoma cells^{8,87}, as well as good clinical response^{10,37,70,107}.

In contrast with PDT, PTT has the advantage that it does not depend on O_2 availability at the treated tumor. Only an efficient mechanism of light-to-heat conversion is necessary in the thermal PS to induce an antitumoral response. The photothermal effect is based on a fast conversion of electronic excitation to vibrational excitation, and then thermal energy is produced from the excited molecule by relaxation of vibrational energy levels^{58,94} (Figure 5).

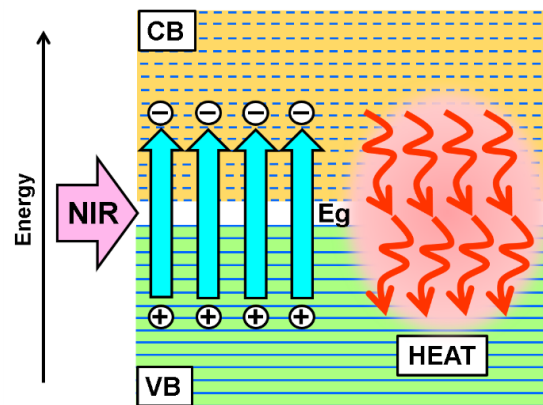


Figure 5. Photothermal effect. The energy of NIR photons is absorbed by electrons in the valence band (VB) of photothermal polymers or nanoparticles, pumping them to the conduction band (CB), through an energy gap (Eg). Electronic excitation leaves positive charges (holes) in the VB, and electrons and holes rapidly recombine converting most of the absorbed energy in lattice vibrations (thermal energy, wiggly arrows).

Photothermal sensitizers such as organic dyes, nanoparticles, and pigments are used in anti-tumoral therapy. Aggregated (stacked) dye and pigment clusters undergo a prompt decay from electronically excited states through a cascade of vibrational (thermal) modes¹⁷. Several cyanine and naphthalocyanine dyes induce damage on cultured tumor cells. Indocyanine green (ICG) has been the PS prototype for PTT using near infrared (NIR) irradiation^{21,127}. Although ICG has been applied for simultaneous PDT and PTT of melanomas⁹⁸, some doubts still exist about the true photothermal or photodynamic mechanism of ICG⁴⁷. Unfortunately, sometimes melanoma cells *in vitro* do not show refringent melanosomes under phase contrast microscopy, and this feature makes it difficult to assess the results of some PDT or PTT treatments.

ICG has been applied for PTT of choroidal melanoma³², and a far-red absorbing cyanine has proved useful for the amelanotic melanoma B78H1 *in vitro* and *in vivo*¹⁷. Some Cu-, Ni-, and Pd-containing dyes show relevant NIR-induced photothermal effects, examples being Cu(II)-hematoporphyrin, Ni(II)-octabutoxy-naphthalocyanine, and Pd(II)-octabutoxy-naphthalocyanine^{17,33}.

Nanoparticles and novel delivery strategies are now increasingly applied for PTT^{70,129}, the most widely used nanomaterials being gold, metal oxides and sulfides, and organic polymers^{55,57,125}. Regarding natural pigments, it is known that photothermal melanin-based hair removal is widely applied in cosmetics⁴⁹. In the case of experimental tumors, pulsed PTT of B16 tumors with broadband incoherent light (600-800 nm) caused vasculature and melanosome damage, with necrosis of tumor cells⁶⁴. Lethal photothermal effects were also observed in murine tumors after PTT with synthetic dopamine-melanin and NIR irradiation^{76,77,128}. China ink (carbon black), carbon nanotubes, and melanin from black sesame seeds and cuttlefish were recently used for NIR-PTT of cell cultures and tumors^{13,44,54}.

Eumelanin is the most suitable endogenous chromophore for direct PTT of melanotic melanoma²⁷. During continuous irradiation with a continuous wave (cw) 808-nm laser a steady heating occurs, with local hyperthermia, macromolecule denaturation, explosive vaporization, cavitation, and shock-wave emission^{5,90}, which result in severe damage of the tumor tissue. Regarding this effect, hyperthermia has been used

for cancer treatment¹⁰⁵. To illustrate this effect, BALB/c mice bearing the experimental melanotic melanoma B16-F10 were subjected to PTT using a cw 808-nm laser irradiation (Figure 6), which produced massive coagulation necrosis, pycnotic nuclei, disrupted tumor cells releasing melanin and cytoplasm fragments²⁷. Epidermal cell damage was not found in the white skin over the NIR irradiated melanoma, even considering that the exciting light had first to traverse this overlaying tissue to reach the tumor.

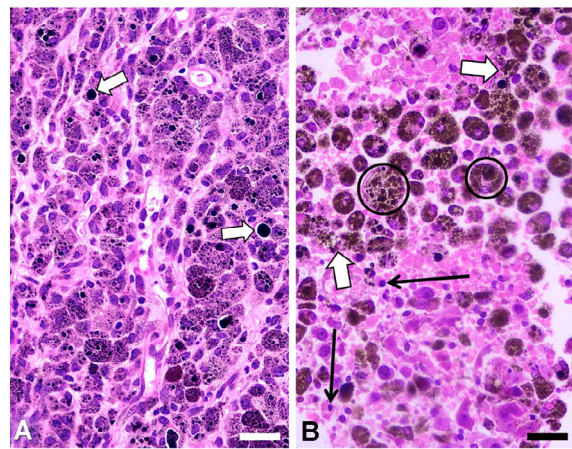


Figure 6. H&E images of paraffin sections from B16-F10 tumors. A: Non-irradiated tumor, with intracellular melanosomes, and large extracellular melanin granules (white arrows). B: Tumor 24 h after NIR irradiation for 10 min with a portable cw 808-nm laser pointer (200 mW, 1.2 mm beam diameter), showing massive necrosis: disrupted tumor cells (white arrows), pycnotic nuclei (black arrows), and large melanophages (encircled). Scale bars: 30 μ m (Reproduced with permission from Colombo *et al.*, Biomedical Optic Express. 2019; 10: 2932-41).

The presence of a great number of brown-black melanophages (Figure 6,B, encircled) is a relevant feature of the irradiated tumor, because these melanin-targeted cells could be subjected to multiple PTT sessions. As glycerol is a strong protecting agent against cell hyperthermia⁵¹, application of a glycerol drop on the depilated skin reduces light scattering caused by keratin and also avoids the non-desired but possible heating and damage of skin tissues.

Absorption and scattering reduce severely light penetration within tissues. On account of deeper tissue penetrance, irradiation with NIR

light at 800-820 nm (the diagnostic and therapeutic window) is commonly used for PTT^{13,27,82}. Using 808-nm PTT, the weak absorbance of melanin is compensated by a deep NIR penetration. Therefore, 808-nm irradiation is very suitable for PTT because the H₂O absorption is negligible, and there are no other absorbing chromophores except melanin^{94,96}. A very efficient electron-phonon coupling occurs in eumelanin²⁹, which explains its rapid decay into heat.

On the other hand, eumelanin shows a high binding capacity for drugs and dyes. Chronic administration of phenothiazine drugs^{16,60} or long-term, high-dose chloroquine therapy⁵³ produced chorioretinopathy, which allowed to suggest an association between toxic effects of some drugs and their high affinity for eumelanin. Likewise, eumelanin binding of drugs has been implicated not only in ocular toxicity, but also in ototoxicity and disturbances of the skin and hair pigmentation⁹⁹. Eumelanin has a strong affinity for certain lipophilic and aromatic compounds, via π - π stacking, electrostatic and van der Waals forces, and/or H-bonding⁸². An example is the binding of eumelanin with the copper phthalocyanine dye Alcian blue 8G²³.

Typical dyes and drugs that bind to eumelanin are acridine orange, aflatoxin B₁, aminoglycoside and tetracycline antibiotics, carcinogenic polycyclic hydrocarbons, chloroquine, chlorpromazine, dexamethasone, diclofenac, fluoroquinolones, herbicides, iodoquine, methotrexate, methylene blue, papaverine, psychotropic and ophthalmic drugs, quinidine, etc.^{50,56,65,68,69,73-75,78,88, 97,102,118}. This striking characteristic of eumelanin can be viewed as an intercalative binding based on hydrophobic and π - π electron interactions, which does not involve structural changes in the X-ray diffraction pattern of the pigment¹¹⁸.

In this proposed intercalative binding mode, the ligand slips between the aromatic units of eumelanin layers and remains trapped as an inclusion complex or "graphitic sandwich", allowing photon-electron-phonon coupling interactions²⁸, which are based on the occurrence of very small HOMO/LUMO energy gaps, as well as pairs of in-phase fused LUMOs (**Figure 7**). Thus, ligand binding to eumelanin results in a greatly improved electric conductivity²³, as well as ultrasonic- and radical/ROS-induced cytotoxicity with preferential killing of melanoma cells^{28,83}.

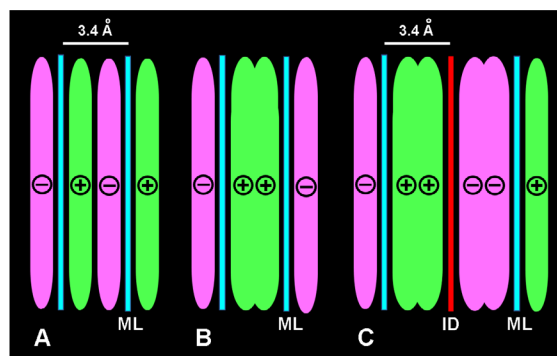


Figure 7. Schematic lateral views of stacked poly BQPo eumelanin layers (ML, blue) showing LUMO patterns, with positive (green) and negative (violet) molecular orbital (MO) lobes of π^* electrons. A: Non-fused MOs at low energy. B: In-phase fused MOs at higher energy. Note the same color and sign of fused MOs. C: In-phase fused LUMOs of two eumelanin layers with an intercalated dye (ID, red). Separation between aromatic planes is indicated.

In keeping with this, several eumelanin-binding dyes could be used as photo- and sono-sensitizing drugs to enhance the antitumoral activity. Suitable chromophores for intercalation between aromatic eumelanin layers are planar vital probes such as some porphyrins, phthalocyanines and porphycenes. Examples would be TMPyP, ZnTPP, Pc13, ZnPc, TPPo, PdTPPo, that accumulate in endosome-lysosome organelles^{115,116}, to which also belong melanosomes¹⁰⁰.

CONCLUSIONS AND PERSPECTIVES

Regarding melanoma and melanin-based PTT, the chemistry of this biopigment is most relevant. The precise molecular structure of eumelanin is still poorly known, but it appears formed by an indole polymer with high conjugation degree. Although several models have been suggested, a linear rigid planar chain formed by BQPo units would be the structure that better explains the unusual physico-chemical properties of melanin and synthetic melanins (e.g., broad-band light absorption, antioxidant capacity, electric conductivity, photothermal effect, and multilayered graphite-like organization).

The high conjugation of the pigment is illustrated by the longitudinal patterns of LUMOs and the reduction of the energy gap between HOMO and LUMO levels. It is logical to assume that on account of its strikingly high

absorption in the UV-visible region, eumelanin is practically the ideal PS for melanoma PTT using NIR (e.g., cw 808-nm laser) irradiation. The massive vibrational decay from photo-excited electronic states induces an immediate and efficient heating response that results in coagulative necrosis of the tumor. As a great amount of melanin is released from melanoma cells during the necrotic process, repetitive NIR treatments are possible due to the remaining melanin contained in intratumoral melanophages.

In addition to its more known biological features, eumelanin also presents a high binding capacity for drugs and dyes with an aromatic and planar configuration. The affinity for such ligands seems to be based on intercalative binding mechanisms through hydrophobic and stacking interactions between planar ligands and aromatic eumelanin layers. In this case, the intercalated ligand remains trapped as an inclusion complex within eumelanin, showing photon-electron-phonon interactions with in-phase fused LUMOs, and reduction of the energy gap.

Ligand binding to eumelanin results in a greatly increased electric conductivity and could improve the photothermal response. As ultrasounds in the 1-MHz range are also strongly absorbed by eumelanin, appropriate ligand-eumelanin complexes could be used as photo- and sono-sensitizing drugs to enhance the antitumoral activity against melanoma cells, by generating increased and selective thermal and radical/ROS cytotoxicity, respectively. In this regard, suitable melanin-binding dyes could be vital probes for lysosomes because melanosomes also belong to these organelles. Therefore, new developments are expected to occur in these innovative fields of physical melanoma therapy.

ACKNOWLEDGEMENTS

I thank A. Blázquez-Castro, L.L. Colombo, L.M.E. Finocchiaro, J. Herkovits, D.M. Lombardo, and M. Pozzi for valuable collaboration.

REFERENCES

1. Abrahamse, H.; Hamblin, M.R. New photosensitizers for photodynamic therapy. *Biochem J.* 2016; 473:347-64.
2. Achkar, T.; Tarhini, A.A. The use of immunotherapy in the treatment of melanoma. *J Hematol Oncol.* 2017; 10:5. DOI 10.1186/s13045-017-0458-3.
3. Ahn, A.; Chatterjee, A.; Eccles, M.R. The slow cycling phenotype: A growing problem for treatment resistance in melanoma. *Mol Cancer Ther.* 2017; 16(6):1002-9.
4. Akasov, R.A.; Sholina, N.V.; Khochenkov, D.A.; *et al.* Photodynamic therapy of melanoma by blue-light photoactivation of flavin mononucleotide. *Sci Reports.* 2019; 9(1):1-11.
5. Angelsky, O.V.; Bekshaev, A.Y.; Maksimyak, P.P. *et al.* Low-temperature laser-stimulated controllable generation of micro-bubbles in a water suspension of absorptive colloid particles. *Opt Exp.* 2018; 26:13995.
6. ArmasPortela, R.; Stockert, J.C. A reaction mechanism for the orthochromatic staining of polysaccharides: monomerizing interactions with basic dyes. *Cell Mol Biol.* 1986; 32:44953.
7. Arzillo, M.; Pezzella, A.; Crescenzi, O.; *et al.* Cyclic structural motifs in 5,6-dihydroxyindole polymerization uncovered: Biomimetic modular buildup of a unique five-membered macrocycle. *Org Lett.* 2010; 12(14):3250-53.
8. Baldea, I.; Filip, A.G. Photodynamic therapy in melanoma - an update. *J Physiol Pharmacol.* 2012; 63(2):109-18.
9. Bancroft, J.D.; Gamble, M. Theory and practice of histological techniques. 6th ed. 2008; Churchill Livingstone, London.
10. Barbazetto, I.A.; Lee, T.C.; Rollins, I.S.; *et al.* Treatment of choroidal melanoma using photodynamic therapy. *Am J Ophthalmol.* 2003; 135(6):898-9.
11. Baskaran, R.; Lee, J.; Yang, S.G. Clinical development of photodynamic agents and therapeutic applications. *Biomaterials Res.* 2018; 22:25.
12. Berrios-Colon, E.; Williams, S. Melanoma review: Background and treatment. *US Pharmacist.* 2012; 37(4): HS-4-HS7.

13. Blázquez-Castro, A.; Colombo, L.L.; Vanzulli, S.I.; Stockert, J.C. NIR pointer laser for *in vivo* photothermal therapy of murine LM3 tumor using intratumoral China ink as a photothermal agent. *Lasers Med Sci.* 2018; 33:1307-15.
14. Blázquez-Castro, A.; Stockert, J.C. Biomedical overview of melanin. 1. Updating melanin biology and chemistry, physico-chemical properties, melanoma tumors, and photothermal therapy. *BIOCELL.* 2021; 45(4):849-62.
15. Bridelli, M.G., Crippa, P.R., Ugozzoli, F. X-ray diffraction studies on melanins in lyophilized melanosomes. *Pigm Cell Res.* 1990; 3:187-91.
16. Burian, H.M.; Fletcher, M.C.; Visual functions in patients with retinal pigmentary degeneration following the use of NP 207. *AMA Arch Ophthalmol.* 1958; 60(4 Part 1):612-29.
17. Camerin, M.; Jori, G.; Della Ciana, L.; *et al.* Photothermal sensitisation and therapeutic properties of a novel far-red absorbing cyanine. *Photochem Photobiol Sci.* 2009; 8:1422-31.
18. Carriel, V.S.; Aneiros-Fernandez, J.; Arias-Santiago, S.; *et al.* A novel histochemical method for a simultaneous staining of melanin and collagen fibers. *J Histochem Cytochem.* 2011; 59:270-7.
19. Cavallini, C.; Vitiello, G.; Adinolfi, B.; *et al.* (2020). Melanin and melanin-like hybrid materials in regenerative medicine. *Nanomaterials* 2020; 10:1518.
20. Cekanova, M.; Rathore, K. Animal models and therapeutic molecular targets of cancer: Utility and limitations. *Drug Des Develop Ther.* 2014; 8:1911-.
21. Chen, W.R.; Adams, R.L.; Higgins, A.K. Photothermal effects on murine mammary tumors using indocyanine green and an 808-nm diode laser: an *in vivo* efficacy study. *Cancer Lett.* 1996; 98:169-73.
22. Chen, Y., Zheng, W., Li, Y., *et al.* Apoptosis induced by methylene-blue mediated photodynamic therapy in melanomas and the involvement of mitochondrial dysfunction revealed by proteomics. *Cancer Sci.* 2008; 99(10): 2019-27.
23. Chen, C.T.; Ball, V.; de Almeida Gracio, J.J.; *et al.* Self-assembly of tetramers of 5,6-dihydroxyindole explains the primary physical properties of eumelanin: experiment, simulation, and design. *ACS Nano* 2013; 7:1524-32.
24. Chen, L.; Malollari, K.G.; Uliana, A.; *et al.* Selective, catalytic oxidations of C–H bonds in polyethylenes produce functional materials with enhanced adhesion. *Chem.* 2021; 7:37-45.
25. Chen, Q.; Xu, L.; Liang, C.; *et al.* Photothermal therapy with immune-adjuvant nanoparticles together with checkpoint blockade for effective cancer immunotherapy. *Nature Comm.* 2016; 7:13193.
26. Cheng, J.; Moss, S.C.; Eisner, M. X-ray characterization of melanins - II. *Pigm Cell Res.* 1994; 7:269-73.
27. Colombo, L.L.; Vanzulli, S.I.; Blázquez-Castro, A.; *et al.* Photothermal effect by 808-nm laser irradiation of melanin: A proof-of-concept study of photothermal therapy using B16-F10 melanotic melanoma growing in BALB/c mice. *Biomed Optics Exp.* 2019; 10:2932-41.
28. Corry, P.M., McGinness, J.E.; Armour, E. Semiconductor properties of melanins related to preferential killing of melanoma cells. *Pigment Cell*, vol. 2, 1976. Karger, Basel, New York. p. 321-26.
29. Crippa, P.R.; Martini, F.; Viappiani, C. Direct evidence of electron-phonon interaction in melanins. *J Photochem Photobiol. B: Biol.* 1991; 11:371-5.
30. D'Alba, L.; Shawkey, M.D. Melanosomes: biogenesis, properties, and evolution of an ancient organelle. *Physiol Rev.* 2019; 99:1-19.
31. Davids, L.M.; Kleemann, B.; Kacerovská, D.; *et al.* Hypericin phototoxicity induces different modes of cell death in melanoma and human skin cells. *J Photochem Photobiol B: Biol.* 2008; 91(2-3):67-76.
32. De Potter, P.; Jamart, J. Adjuvant indocyanine green in transpupillary thermotherapy for choroidal melanoma. *Ophthalmology.* 2003; 110:406-13.
33. Diddens, H.; Fischer, F.; Pottier, R.H. *In-vivo* investigations on dye-enhanced photothermal tumor therapy with a naphthalocyanine derivative. *Oftalmologia.* 2003; 56(1):59-61.
34. d'Ischia, M.; Napolitano, A.; Pezzella, A.; *et al.* Melanin biopolymers: tailoring chemical complexity for materials design. *Angew Chem Int Ed.* 2019. DOI 10.1002/anie.201914276.

35. d'Ischia, M.; Wakamatsu, K.; Cicoira, F.; *et al.* Melanins and melanogenesis: from pigment cells to human health and technological applications. *Pig Cell Melan Res.* 2015; 28:520-44.
36. Domingues, B.; Lopes, J.M.; Soares, P.; Pópulo, H. Melanoma treatment in review. *Imm Targ Therapy.* 2018; 7:35-49.
37. Donaldson, M.J.; Lim, L.; Harper, C.A.; *et al.* (2005). Primary treatment of choroidal amelanotic melanoma with photodynamic therapy. *Clin Exp Ophthalmol.* 2005; 33(5):548-49.
38. Dreyer, D.R.; Miller, D.J.; Freeman, B.D.; *et al.* Elucidating the structure of poly(dopamine). *Langmuir.* 2012; 28:6428-35.
39. Dysli, C.; Wolf, S.; Berezin, M.Y.; *et al.* Fluorescence lifetime imaging ophthalmoscopy. *Prog Retin Eye Res.* 2017; 60:120-43.
40. Fellner, M.J.; Chen, A.S.; Mont, M.; *et al.* Patterns and intensity of autofluorescence and its relation to melanin in human epidermis and hair. *Int J Dermatol.* 1979; 18(9):722-30.
41. Fernandes, B.; Matamá T.; Guimaraes, D.; *et al.* Fluorescent quantification of melanin. *Pigm Cell Melan Res.* 2016; 29(6):707-12.
42. Finocchiaro, L.M.E.; Fondello, C.; Gil-Cardeza, M.L. Cytokine-enhanced vaccine and interferon- β plus suicide gene therapy as surgery adjuvant treatments for spontaneous canine melanoma. *Human Gene Ther.* 2015; 26:367-76.
43. Finocchiaro, L.M.E.; Agnetti, L.; Fondello, C.; Glikin, G.C. Combination of cytokine-enhanced vaccine and chemo-gene therapy as surgery adjuvant treatments for spontaneous canine melanoma. *Gene Ther.* 2019; 26:418-31.
44. Fisher, J.W.; Sarkar, S.; Buchanan, C.F.; *et al.* Photothermal response of human and murine cancer cells to multiwalled carbon nanotubes after laser irradiation. *Cancer Res.* 2010; 70:9855-64.
45. Galeb, H.A.; Wilkinson, E.L.; Stowell, A.F.; *et al.* Melanins as sustainable resources for advanced biotechnological applications. *Global Chall.* 2021; 5:2000102.
46. Gallas, J.M.; Eisner, M.; Fluorescence of melanin-dependence upon excitation wavelength and concentration. *Photochem Photobiol.* 1987; 45(5):595-600.
47. Giraudeau, C.; Moussaron, A.; Stallivieri, A. Indocyanine green: photosensitizer or chromophore? Still a debate. *Curr Med Chem.* 2014; 21:1871-97.
48. Grube, D. Immunoperoxidase methods: Increased efficiency using fluorescence microscopy for 3,3-diaminobenzidine (DAB) stained semithin sections. *Histochem.* 1980; 70(1):19-22.
49. Haedersdal, M.; Beerwerth, F.; Nash, J.F. (2011). Laser and intense pulsed light hair removal technologies: from professional to home use. *Br J Dermatol.* 2011; 165(Suppl 3):31-6.
50. Hellinen, L.; Bahrpeyma, S.; Rimpelä, A.K.; *et al.* Microscale thermophoresis as a screening tool to predict melanin binding of drugs. *Pharmaceutics.* 2020; 12:554.
51. Henle, K.J.; Warters, R.L. Heat protection by glycerol *in vitro*. *Cancer Res.* 1982; 42:2171-76.
52. Hill, H.Z. The function of melanin or six blind people examine an elephant. *Bioessays.* 1992; 14:49-56.
53. Hobbs, H.E.; Sorsby, A.; Freedman, A. Retinopathy following chloroquine therapy. *Lancet.* 1959; 274(7101):478-80.
54. Huang, L.; Liu, M.; Huang, H.; *et al.* Recent advances and progress on melanin-like materials and their biomedical applications. *Biomacromolecules.* 2018; 19:1858-68.
55. Huang, X.; El-Sayed, I.H.; Qian, W.; El-Sayed, M.A. Cancer cell imaging and photothermal therapy in the near-infrared region by using gold nanorods. *J Am Chem Soc.* 2006; 128(6): 2115-20.
56. Jakubiak, P.; Cantrill, C.; Urtti, A.; Alvarez-Sánchez, R. Establishment of an *in vitro-in vivo* correlation for melanin binding and the extension of the ocular half-life of small-molecule drugs. *Mol Pharmaceutics.* 2019; 16:4890-901.
57. Jiang, R.; Cheng, S.; Shao, L.; Ruan, Q. Mass-based photothermal comparison among gold nanocrystals, PbS nanocrystals, organic dyes, and carbon black. *J Phys Chem C.* 2013; 117:8909-15.

58. Jori, G.; Spikes, J.D. Photothermal sensitizers: possible use in tumor therapy. *J Photochem Photobiol B: Biol.* 1990; 6:93-101.
59. Kayatz, P.; Thumann, G.; Luther, T.T.; *et al.* Oxidation causes melanin fluorescence. *Invest Ophthalmol Vis Sci.* 2001; 42(1):241-6.
60. Kinross-Wright, V. Clinical trial of a new phenothiazine compound: NP-207. *Psych Res Rep.* 1956; 4:89-94.
61. Kolarova, H.; Nevrelova, P.; Bajgar, R.; *et al.* *In vitro* photodynamic therapy on melanoma cell lines with phthalocyanine. *Toxicol in Vitro.* 2007; 21(2):249-53.
62. Kono, R.; Yamaoka, T.; Yoshizaki, H.; John McGinness, J. Anomalous absorption and dispersion of sound waves in diethylamine melanin. *J Appl Phys.* 1979; 50:1236-44.
63. Kono, R.; Yoshizaki, H. Ultrasonic shear spectrum in hydrated diethylamine melanins and its relation to stacking in a planar group. *J Chem Phys.* 1981; 75:4654.
64. Kostenich, G.; Babushkinab, T.; Malikb, Z.; Orenstein, A. Photothermic treatment of pigmented B16 melanoma using a broadband pulsed light delivery system. *Cancer Lett.* 2000; 157:161-68.
65. Kowalska, J.; Banach, K.; Rok, J.; *et al.* Molecular and biochemical basis of fluoroquinolones-induced phototoxicity—The study of antioxidant system in human melanocytes exposed to UV-A radiation. *Int J Mol Sci.* 2020, 21:9714.
66. Krol, E.S.; Liebler, D.C. Photoprotective actions of natural and synthetic melanins. *Chem. Res. Toxicol.* 1998; 11:1434-40.
67. Kuzu, O.F.; Nguyen, F.D.; Noory, M.A.; Sharma, A. Current state of animal (mouse) modeling in melanoma research. *Cancer Growth Metast.* 2015; 8s1:81-94.
68. Larsson, B.S. Melanin-affinic thioureas as selective melanoma seekers. *Melanoma Res.* 1991; 1(2):85-90.
69. Larsson, B.S. Interaction between chemicals and melanin. *Pigm Cell Res.* 1993; 6(3):127-33.
70. Li, Z.; Yu, X.F.; Chu, P.K. Recent advances in cell-mediated nanomaterial delivery systems for photothermal therapy. *J Mat Chem. B.* 2018; 6:1296-311.
71. Li, X.Y.; Tan, L.C.; Dong, L.W.; *et al.* Susceptibility and resistance mechanisms during photodynamic therapy of melanoma. *Front Oncol.* 2020; 10:1-17.
72. Liebscher, J.; Mrówczyński, R.; Scheidt, H.A.; *et al.* Structure of polydopamine: A never-ending story? *Langmuir.* 2013; 29:10539-48.
73. Lindquist, N.G.; Ullberg, S. (1972). The melanin affinity of chloroquine and chlorpromazine studied by whole body autoradiography. *Acta Pharm Toxicol.* 1972; 1:1-32.
74. Lindquist, N.G. Accumulation of drugs on melanin. *Acta Radiol Diagn.* (Stockh). 1973; 325:1-92.
75. Link, E.; Łukiewicz, S. A new radioactive drug selectively accumulating in melanoma cells. *Eur J Nucl Med.* 1982; 7(10):469-73.
76. Liu, Y.; Ai, K.; Liu, J.; *et al.* Dopamine-melanin colloidal nanospheres: an efficient near infrared photothermal therapeutic agent for *in vivo* cancer therapy. *Adv Mater.* 2013; 25:1353-59.
77. Liu, Y.; Ai, K.; Lu, L. Polydopamine and its derivative materials: Synthesis and promising applications in energy, environmental, and biomedical fields. *Chem Rev.* 2014; 114(9):5057-115.
78. Lowrey, A.H., Fameini, G.R., Loumbev, V., *et al.* Modeling drug-melanin interaction with theoretical linear solvation energy relationships. *Pigm Cell Res.* 1997; 10(5):251-56.
79. Maduray, K.; Karsten, A.; Odhav, B.; Nyokong, T. *In vitro* toxicity testing of zinc tetrasulfophthalocyanines in fibroblast and keratinocyte cells for the treatment of melanoma cancer by photodynamic therapy. *J Photochem Photobiol B: Biol.* 2011; 103(2):98-104.
80. Marino, J.; García Vior, M.C.; Furmento, V.A.; *et al.* Lysosomal and mitochondrial permeabilization mediates zinc(II) cationic phthalocyanine phototoxicity. *Int J Biochem Cell Biol.* 2013; 45(11):2553-62.
81. Martínez, L.M.; Martínez, A.; Gosse, G. Production of melanins with recombinant microorganisms. *Front Bioeng Biotechnol.* 2019; 7:285.
82. Mavridi-Printezi, A.; Guernelli, M.; Menichetti, A.; Montalti, M. Bio-applications of multifunctional

- melanin nanoparticles: From nanomedicine to nanocosmetics. *Nanomaterials*. 2020; 10:2276.
83. McGinness, J.E.; Corry, P.M.; Armour, E. Melanin-binding drugs and ultrasonic-induced cytotoxicity. *Pigment Cell*, vol. 2, 1976. Karger, Basel, New York. p. 316-20.
 84. Meng, S.; Kaxiras, E. Theoretical models of eumelanin protomolecules and their optical properties. *Biophys J*. 2008; 94:2095-105.
 85. Meredith, P.I.; Riesz, J. Radiative relaxation quantum yields for synthetic eumelanin. *Photochem Photobiol*. 2004; 79(2):211-6.
 86. Micillo, R.; Panzella, L.; Koike, K.; *et al.* "Fifty shades" of black and red or how carboxyl groups fine tune eumelanin and pheomelanin properties. *Int J Mol Sci*. 2016; 17:746.
 87. Naidoo, C.; Kruger, C.; A. Abrahamse, H. Photodynamic therapy for metastatic melanoma treatment: A review. *Technol Cancer Res Treat*. 2018; 17:1-15.
 88. Napolitano, A.; Palumbo, A.; d' Ischia, M.; Prota, G. Mechanism of selective incorporation of the melanoma seeker 2-thiouracil into growing melanin. *J Med Chem*. 1996; 39(26):5192-201.
 89. Nicolaus, R.A. Coloured organic semiconductors: melanins. *Rend Accad Sci Fis Mat*. 1997; 64:325-60.
 90. Olivieri, M.; Nicolaus, R.A. Sulla DHI-melanina. *Rend Accad Sci Fis Mat*. 1999; 66:85-96.
 91. Overwijk, W.W.; Restifo, N.P. B16 as a mouse model for human melanoma. *Curr Prot Immunol*. 2000; 39(1):20.1.
 92. Panzella, L.; Ebato, A.; Napolitano, A.; Koike, K. The late stages of melanogenesis: Exploring the chemical facets and the application opportunities. *Int J Mol Sci*. 2018; 19: 1753.
 93. Park, J.; Moon, H.; Hong, S. Recent advances in melanin-like nanomaterials in biomedical applications: a mini review. *Biomat Res*. 2019; 23:24.
 94. Parrish, J.A.; Anderson, R.R.; Harrist, T.; *et al.* Selective thermal effects with pulsed irradiation from lasers: From organ to organelle. *J Invest Dermatol*. 1983; 80(6 supplement):75s-80s.
 95. Pereira, N.A.M.; Laranjo, M.; Pina, J.; *et al.* Advances on photodynamic therapy of melanoma through novel ring-fused 5,15-diphenylchlorins. *Eur J Med Chem*. 2018; 146:395-408.
 96. Plaetzer, K.; Krammer, B; Berlanda, J.; *et al.* Photo-physics and photochemistry of photodynamic therapy: fundamental aspects. *Lasers Med Sci*. 2009; 24:259-68.
 97. Potts, A.M. Uveal pigment and phenothiazine compounds. *Trans Am Ophthal Soc*. 1962; 60:517-52.
 98. Radzi, R.; Osaki, T.; Tsuka, T.; *et al.* Morphological study in B16F10 murine melanoma cells after photodynamic hyperthermal therapy with indocyanine green (ICG). *J Vet Med Sci*. 2012; 74(4):465-72.
 99. Raghavan, P.R.; Zane, P.A.; Tripp, S.L. Calculation of drug-melanin binding energy using molecular modeling. *Experientia*. 1990; 46(1):77-80.
 100. Raposo, G.; Marks, M.S. Melanosomes — dark organelles enlighten endosomal membrane transport. *Nature Rev Mol Cell Biol*. 2007; 8(10):786-97.
 101. Rapozzi, V.; Zorzet, S.; Zacchigna, M.; *et al.* (2014). Anticancer activity of cationic porphyrins in melanoma tumour-bearing mice and mechanistic *in vitro* studies. *Mol Cancer*. 2014; 13(1):1-17.
 102. Rimpelä, A.K.; Garneau, M.; Baum-Kroger, K.S.; *et al.* Quantification of drugs in distinctly separated ocular substructures of albino and pigmented rats. *Pharmaceutics*. 2020; 12:1174.
 103. Rughani, M.G.; Gupta, A.; Middleton, M.A. New treatment approaches in melanoma: current research and clinical prospects. *Ther Adv Med Oncol*. 2013; 5(1):73-80.
 104. Ruiz-Molina, D.; Saiz Poseu, J.; Busque, F.; *et al.* The chemistry behind catechol-based adhesion. *Ang Chem Int Ed*. 2018; DOI 10.1002/anie.201801063.
 105. Sethi, M.; Chakarvarti, S.K. Hyperthermia techniques for cancer treatment: A review. *Int J Pharm Tech Res*. 2015; 8(6):292-9.
 106. Scognamiglio, F.; Travan, A.; Turco, G.; *et al.* Adhesive coatings based on melanin-like nanoparticles for surgical membranes. *Coll Surf B: Bioint*. 2017; DOI 10.1016/j.colsurfb.2017.04.057.

107. Sheleg, S.V.; Zhavrid, E.A.; Khodina, T.V.; *et al.* Photodynamic therapy with chlorin e6 for skin metastases of melanoma. *Photodermatol Photoimmunol Photomed.* 2004; 20(1): 21-6.
108. Skidan, I.; Dholakia, P.; Torchilin, V.P. Photodynamic therapy of experimental B-16 melanoma in mice with tumor-targeted 5,10,15,20-tetraphenylporphin-loaded PEG-PE micelles. *J Drug Target.* 2008; 16(6):486-93.
109. Smith, S.H.; Goldschmidt, M.H.; McManus, P.M. A comparative review of melanocytic neoplasms. *Vet Pathol.* 2002; 39:651-78.
110. Sniegocka, M.; Podgórska, E.; Płonka, P.M.; *et al.* Transplantable melanomas in hamsters and gerbils as models for human melanoma. Sensitization in melanoma radiotherapy—From animal models to clinical trials. *Int J Mol Sci.* 2018; 19:1048.
111. Solano, F. Melanin and melanin-related polymers as materials with biomedical and biotechnological applications—Cuttlefish ink and mussel foot proteins as inspired biomolecules. *Int J Mol Sci.* 2017; 18:1561.
112. Stockert, J.C. Cytochemistry of nucleic acids: binding mechanisms of dyes and fluorochromes. *Micr Electr Biol Cel.* (BIOCELL). 1985; 9:89-131.
113. Stockert JC, Blázquez-Castro A. Fluorescence microscopy in life sciences, E-Book, Bentham Science Publishers, Sharjah, U.A.E. 2017.
114. Stockert, J.C.; Cañete, M.; Colman, O.D. Histochemical mechanism for the orthochromatic staining and fluorescence reaction of lignified tissues. *Cell Mol Biol.* 1984; 30:503-8.
115. Stockert, J.C.; Cañete, M.; Juarranz, A.; *et al.* Porphyrines: facts and prospects in photodynamic therapy of cancer. *Curr Med Chem.* 2007; 14:997-1026.
116. Stockert, J.C.; Juarranz, A.; Villanueva, A.; *et al.* Photodynamic therapy: selective uptake of photosensitizing drugs into tumor cells. *Curr Top Pharmacol.* 2004; 8:185-217.
117. Stockert, J.C.; Herkovits, J. Melanin adhesivity for possible trapping of SARS-CoV-2 on chin straps: a proof-of-concept assay using model nanoparticles. *Acta Sci. Microbiol.* 2021; 4:2-5.
118. Thathachari, Y.T.; Blois, M.S. Physical studies on melanins. II. X-ray diffraction. *Biophys J.* 1969; 6:77-89.
119. Toubia, I.; Nguyen, C.; Diring, S.; *et al.* Study of cytotoxic and photodynamic activities of dyads composed of a zinc phthalocyanine appended to an organotin. *Pharmaceuticals.* 2021; 14:413.
120. Valli, F.; García Vior, M.C.; Roguin, L.P.; Marino, J. Oxidative stress generated by irradiation of a zinc(II) phthalocyanine induces a dual apoptotic and necrotic response in melanoma cells. *Apoptosis.* 2019; DOI 10.1007/s10495-018-01512-w.
121. Wang, Y.; You, W.; LI, X. Current status of gene therapy in melanoma treatment. *BIOCELL.* 2020; 44(2):167-74.
122. Wang, Z.; Peng, H.; Shi, W.; *et al.* Application of photodynamic therapy in cancer: challenges and advancements. *BIOCELL.* 2021; 45(3):489-500.
123. Watt, A.A.R.; Bothma, J.P.; Meredith, P. The supramolecular structure of melanin. *Soft Matter.* 2009; 5:3754-60.
124. Whittingham, M.S.; Jacobson, A.J., Editors. Intercalation chemistry. Academic Press, New York, London, 1982.
125. Yue, Y.; Zhao, X. Melanin-like nanomedicine in photothermal therapy applications. *Int J Mol Sci.* 2021; 22(1):399.
126. Zajac, G.W.; Gallas, J.M.; Cheng, J.; *et al.* The fundamental unit of synthetic melanin: a verification by tunneling microscopy of X-ray scattering results. *Biophys Biochim Acta.* 1994; 1199:271-8.
127. Zheng, X.; Xing, D.; Zhou, F.; *et al.* Indocyanine green-containing nanostructures as near infrared dual-functional targeting probes for optical imaging and photothermal therapy. *Mol Pharmaceutics.* 2011; 8(2):447-56.
128. Zheng, R.; Wang, S.; Tian, Y.; *et al.* Polydopamine-coated magnetic composite particles with an enhanced photothermal effect. *ACS Appl Mat Interf.* 2015; 7:15876-84.
129. Zhou, X.; McCallum, N.C.; Hu, Z.; *et al.* Artificial allomelanin nanoparticles. *ACS Nano.* 2019; DOI 10.1021/acsnano.9b02160.